Phase boundaries near critical end points. II. General spherical models

Marcia C. Barbosa* and Michael E. Fisher
Institute for Physical Science and Technology, University of Maryland, College Park, Maryland 20742
(Received 21 December 1990)

We study d-dimensional ferromagnetic spherical models with power-law, $J(R)\sim 1/R^{d+\sigma}$ ($\sigma<2$), or short-range ($\sigma\cong 2$) interactions and on-site terms of the form $Ds^2-|U|s^4+Vs^6$, and establish that the phase diagrams for all d and σ with $\sigma<d<2\sigma$, may exhibit *critical end points* terminating *nonclassical* critical lines; tricritical points may arise only for $\frac{3}{2}\sigma\le d$. The phase boundary $D_\sigma(T,h)$, where h is the magnetic field, between the noncritical, spectator phase and the ordering and critical phase is shown to exhibit singularities at the end point with amplitudes obeying the universal ratio laws advanced on phenomenological grounds in Part I.

I. INTRODUCTION

In Ref. 1 (to be referred to hereafter as I) the nature of the phase boundaries in the vicinity of a critical end point was considered. To be concrete, we may suppose that there is a transition of Ising-like character ($n=1$), in which case two distinct phases β and γ may coexist on a manifold ρ in a basic thermodynamic space of three field variables (T,g,h); see Figs. 1 and 2 of I.[1] For an order parameter of symmetry $O(n)$ with $n\ge 2$, the ordered phase on ρ has a sense and may be denoted $\vec{\beta}_-$ (see I). In both cases $h(\equiv|\vec{h}|)$ is an ordering field for the transition, while g is a nonordering field;[2-4] the manifold ρ is thus a segment of the $h=0$ or (T,g) plane. For simplicity we will consider here only the situation which is fully symmetric under $\vec{h}\to-\vec{h}$.

As T increases, we suppose that the phases β and γ for $n=1$ (or $\vec{\beta}_-$ for $n\ge 2$) approach criticality on a λ line $T_\lambda(g)$ (see I, Fig. 1), where they merge to form a disordered phase $\beta\gamma$ for $n=1$ (or β_+ for $n\ge 2$). When a critical end point is present, the planar manifold ρ meets a phase boundary σ which demarcates a new, noncritical or spectator phase α, stable, say, at low g; see I, Fig. 2.[2] The line of intersection between ρ and σ in the $h=0$ plane τ is a triple line on which all three phases α, β, and γ may coexist for $n=1$ (or phases α and $\vec{\beta}_-$ for $n\ge 2$). The triple line τ terminates where it meets the critical line λ *at the critical end point* $[T_e=T_c(g_e),\ g_e,\ h=0]$.

In I we addressed the question: What sort of singularities, if any, should be observed near the critical end point in the function $g_\sigma(T,h)$, which specifies the phase boundary σ to the spectator phase α? On the basis of phenomenological and thermodynamic considerations, we argued that $g_\sigma(T,h)$ should display characteristic nonanalyticities at the critical end point controlled by the bulk critical properties of the β, γ, and $\beta\gamma$ phases on the critical line λ.[1,3,4] Thus it was concluded, for example, that for small

$$\hat{t}\equiv(T-T_e)/T_0\ , \tag{1.1}$$

where T_0 is a convenient reference temperature, the phase boundary σ should vary as

$$g_\sigma(T,h)\approx g_e+g_1\hat{t}-X_\pm|\hat{t}|^{2-\alpha}-Y_\pm|\hat{t}|^\beta|h| -\tfrac{1}{2}Z_\pm|\hat{t}|^{-\gamma}h^2+\Delta g_0(T,h)\ , \tag{1.2}$$

when $h\to 0$, with $Y_+\equiv 0$, and where α, β, and γ are the (universal) critical exponents characterizing the λ line.[5] The function $\Delta g_0(T,h)$ contains nonsingular terms quadratic in $\hat{t}$ and h and singular terms of $O(h^3)$. Furthermore, it was demonstrated that appropriate dimensionless ratios of the amplitudes, $X_\pm$, $Y_\pm$, and $Z_\pm$ should have universal values directly determined by various *bulk* amplitude ratios *on* the λ line. Specifically, if $A_\pm$, B, and $C_\pm$ are the amplitudes for the specific heat, spontaneous order $M_0(T)$, and susceptibility on the λ line, then the ratios

$$X_-/X_+=A_-/A_+,\quad Z_-/Z_+=C_-/C_+\ , \tag{1.3}$$

$$\Xi_1\equiv\frac{X_+Z_+}{Y_-^2}=\frac{A_+C_+}{(2-\alpha)(1-\alpha)B^2}\ , \tag{1.4}$$

together with similar expressions for the field behavior on the end-point isotherm $T=T_e$, etc.,[1] should all be universal.

Now the arguments in I leading to (1.1)–(1.4), etc., were plausible but nonrigorous. They assumed that no new type of criticality arises at an end point, and they ignored the effects of counterphase or droplet fluctuations that might, possibly, induce such changes and which surely do lead to singularities in the free energy, etc., as the phase boundary σ is approached at *or* away from (T_e,g_e).[6] Accordingly, I stressed the importance of checking these assumptions and the predictions (1.1)–(1.4), etc., by analytic calculations for specific models exhibiting critical end points on nonclassical critical lines. Such an analysis is presented in this paper.

Explicitly, we consider a general class of d-dimensional spherical models, or n-vector models in the limit $n\to\infty$,[7,8] which have either short-range couplings or long-range, power-law interactions. These models were originally studied by Sarbach and Fisher[9,10] (following

earlier work by Sarbach and Schneider[11] and by Emery[7]) because they displayed nontrivial *tricritical points.*[12] We show here that for *all* dimensionalities and forms of interaction they *also* display critical lines which terminate at *critical end points* (instead of tricritical points) for suitable values of the parameters in the Hamiltonian. This actually contradicts an assertion of Ref. 11 to the effect that only tricritical points occur above a certain dimensionality d_0, equal to 3 for short-range interactions. Indeed, the elucidation of the various types of phase diagrams displayed by the models is an interesting feature of our analysis; see the figures below. For $d<4$, *nonclassical* critical end points arise; for these we show here by detailed calculations that the phase boundary σ is indeed described by (1.1), (1.2), etc., with universal amplitude ratios (restricted somewhat in the light of special features of the spherical model) given by (1.3), (1.4), etc. In higher dimensions, the leading critical behavior is classical; however, there are corrections to scaling which are also reflected in the phase boundary near end points. This aspect is reserved for a future paper to be referred to here as paper III.[13]

In outline, the balance of the paper is as follows: Sec. II describes the model and its known features following closely Sarbach and Fisher;[9] references to equations in that paper are prefixed by SF. The phase diagrams realized are discussed in Sec. III: see Figs. 1–6 below. The free energy near the λ line is analyzed in Sec. IV and the critical amplitudes are evaluated. In Sec. V the free energy of the spectator phase is discussed and the end point parameters are determined in various regimes. Finally, in Sec. VI the predictions (1.3) and (1.4), and their analogs on the critical isotherm are checked and found to be valid. A few concluding remarks close the section. The Appendix discusses the behavior of the basic correlation integral which is needed to higher order than usual.

II. SPHERICAL MODELS WITH SIXTH-ORDER TERMS

A. The model

Following SF,[9] we consider a regular d-dimensional lattice with sites $i=1,2,\ldots,N$ occupied by n-component spins $\mathbf{s}_i$, and posit the Hamiltonian.

$$\mathcal{H}=\tfrac{1}{2}\sum_{(ij)} J_{ij}|\vec{s}_i-\vec{s}_j|^2-\sum_{i=1}^{N}[\vec{h}\cdot\vec{s}_i-nW(|\vec{s}_i|^2/n)]\ , \tag{2.1}$$

where the "on-site" term is of sixth order, with

$$W=\tfrac{1}{2}D|\vec{s}_i|^2+\tfrac{1}{4}U|\vec{s}_i|^4/n+\tfrac{1}{6}V|\vec{s}_i|^6/n^2\ . \tag{2.2}$$

The quadratic coupling coefficient D will play the role of the thermodynamic nonordering field g of Sec. I.[2] The regime of interest, which allows both tricriticality and nonclassical end points, is

$$U<0,\quad V>0,\quad \text{so } w\equiv -U/2V>0\ . \tag{2.3}$$

The first sum in (2.1) runs over all lattice-site pairs (i,j). The interaction energy $J_{ij}=J(\mathbf{R}_{ij})$ will be specified by its Fourier transform

$$\hat{J}(\mathbf{k})=\sum_{\mathbf{R}} e^{i\mathbf{k}\cdot\mathbf{R}}J(\mathbf{R})\ . \tag{2.4}$$

Specifically, we suppose $\hat{J}(\mathbf{k})$ has a unique maximum at $\mathbf{k}=0$, about which

$$\hat{J}(\mathbf{k})=\hat{J}(\mathbf{0})-\hat{J}_\sigma|\mathbf{k}a|^\sigma+\cdots\ , \tag{2.5}$$

where a denotes the lattice spacing, $\hat{J}_\sigma>0$, and $0<\sigma\le 2$. (See also the Appendix.) The value $\sigma=2$ describes short-range interactions; for $\sigma<2$, one has long-range couplings with $J(\mathbf{R})\sim 1/R^{d+\sigma}$ as $R\to\infty$.

B. The free energy

In the thermodynamic limit $N\to\infty$ and the spherical model limit $n\to\infty$, the free energy per spin component is given by SF (2.6), (3.13), etc., as

$$F(T,D,h)=\min_{m_2}\{\tfrac{1}{2}k_BT[\mathcal{I}_d(\zeta)-\zeta I_d(\zeta)]+W(m_2)-hm\}\ , \tag{2.6}$$

where $h=|\vec{h}|$, while

$$m=\langle s\rangle\quad\text{and}\quad m_2=\langle s^2\rangle \tag{2.7}$$

are the two basic thermodynamic densities beyond the energy. The spherical field $\zeta(T,D,h)$ is determined by the *constraint equation*

$$m_2=k_BTI_d(\zeta)+m^2\ , \tag{2.8}$$

and, by minimization of m_2, the *equation of state* is

$$\zeta=h/m=D+Um_2+Vm_2^2\ . \tag{2.9}$$

Finally, the underlying free energy and correlation integrals are defined by SF (2.8) and (2.9) as

$$\mathcal{I}_d(\zeta)=\int\frac{a^d d^dk}{(2\pi)^d}\ln\{[\zeta+\hat{J}(\mathbf{0})-\hat{J}(\mathbf{k})]/2\pi k_BT\}\ , \tag{2.10}$$

in which the integral runs over an appropriate Brillouin zone, while

$$I_d(\zeta)=\frac{\partial\mathcal{I}_d}{\partial\zeta}\ . \tag{2.11}$$

For purposes of estimation we may usually approximate the Brillouin zone by a sphere of radius $|\mathbf{k}|=\bar{\pi}/a$ with $\bar{\pi}\simeq\pi$.

C. Critical behavior

To understand the critical behavior of spherical models it is crucial to know the variation of $\mathcal{I}_d$ and I_d as $\zeta\to 0$. This, in turn, depends strongly on the dimensionality. It is convenient to define upper and lower borderline dimensions $d_\pm$ and an intermediate dimension d_0 via

$$d_-\equiv\sigma<d_0\equiv\tfrac{3}{2}\sigma<d_+\equiv 2\sigma\ . \tag{2.12}$$

We will consider only $d>d_-$; then $I_d(0)\equiv I_d^0$ is a well-defined positive number. The nonclassical regime is specified by $d_-<d<d_+$, and in this range one finds (subject to some conditions explained in the Appendix)

$$I_d(\zeta)=I_d^0[1-p\zeta^{1/\gamma}+q\zeta+o(\zeta)]\ , \tag{2.13}$$

where the susceptibility exponent is given by

$$\gamma=\sigma/(d-\sigma)\geq 1 \quad (0<\sigma\leq 2) \tag{2.14}$$

while p and q are positive coefficients. The combination

$$I_d^0\hat{J}_\sigma^{1+(1/\gamma)}p=1/2^{d-1}\pi^{(d-2)/2}\sigma\Gamma(d/2)\sin(\pi/\gamma)\ , \tag{2.15}$$

has a universal value, while q depends on the details of the interactions but may be estimated by

$$I_d^0\hat{J}_\sigma^{2}q\simeq\gamma/2^{d-1}\pi^{d/2}\sigma\Gamma(d/2)(\gamma-1)\tilde{\pi}^{2\sigma-d}\ , \tag{2.16}$$

in which, as before, $\tilde{\pi}\simeq\pi$: see the Appendix. In the usual asymptotic analysis of the spherical model[8–11,14] only the leading ζ dependence is needed in (2.13). It transpires, however, that to elucidate the behavior when end points arise requires the next correction as well.

All other critical exponents of the spherical model follow from (2.13).[14] For completeness we quote

$$\alpha=1-\gamma,\quad \beta=\tfrac{1}{2},\quad \delta=2\gamma+1\ ,$$
$$\Delta=\gamma+\tfrac{1}{2},\quad \nu=\tfrac{1}{2}\gamma,\quad \eta=0\ . \tag{2.17}$$

These values satisfy all the scaling and, for $d<d_+$, hyperscaling relations. Above d_+ the exponents take their classical values [corresponding to $\gamma=1$ in (2.17)]. On the borderline $d=d_+$, logarithmic factors enter into the susceptibility and specific heat,[14] but we reserve that case for paper III. It will be convenient to treat d, γ, and σ as continuous variables, although the reader is free to keep d as an integer and vary only σ or, equivalently, γ.

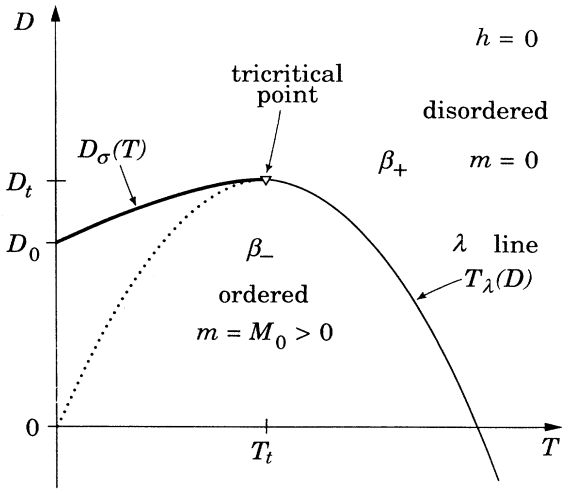

FIG. 1. Phase diagram for the general spherical model with Hamiltonian (2.1)–(2.3) when $h=0$ in the regime of "simple" tricriticality. The conditions under which this diagram applies are discussed in the text. The location (T_t,D_t) of the tricritical point is marked here and in subsequent figures by an inverted triangle. It lies on the λ line $T_\lambda(D)$, which is characterized by nonclassical exponents. The λ line is parabolic in shape; its analytic extension below T_t is shown as a dotted line. The first-order phase boundary $D_\sigma(T)$ below T_t is represented by a bold line; it separates a disordered β_+ phase with $m=\langle s\rangle=0$ from an ordered phase β_- with a spontaneous order $M_0>0$.

D. Lambda line and tricritical point

By (2.9), ζ approaches χ^{-1}, the inverse susceptibility, as $h\to 0$ in a disordered phase with $m(h\to 0)=0$. Criticality with $\chi\to\infty$ is thus confined, via (2.8) and (2.9), to a parabolic locus given by

$$k_BT_\lambda(D)=[|U|+(U^2-4VD)^{1/2}]/2VI_d^0\ , \tag{2.18}$$

as shown in Fig. 1. Note that we use the notation T_λ rather than T_c as in I because a new critical point, not on the λ line, will appear in association with all end points.

In the simplest situation, studied extensively by SF, the vertex of this parabola is a *tricritical point* with parameters

$$k_BT_t=\frac{w}{I_d^0},\quad D_t=\tfrac{1}{4}\frac{U^2}{V},\quad h_t=0,\quad m_{2,t}=w\equiv\tfrac{1}{2}\frac{|U|}{V}\ , \tag{2.19}$$

as indicated in Fig. 1. A first-order phase boundary $D_\sigma(T,h=0)$, across which both $m_0\equiv\lim_{h\to 0+}m(h,T)$ and m_2 change discontinuously, leaves the tricritical point with a horizontal tangent; it intersects the $T=0$ axis at $D_0=3U^2/16V$: see Fig. 1.

For small D the critical or λ line is always present. However, at larger values of $D<D_t$ it may happen that another phase becomes preferred, that is, has a lower free energy than the critical phase. In that case the tricritical point will *not* be realized in an equilibrium phase diagram. Rather, the λ line will be cut off by a *critical end point* at some $D_e<D_t$ and $T_e=T_\lambda(D_e)>T_t$. In the next section we discuss when that happens and, more generally, determine how the phase diagram may differ from Fig. 1. If there *is* a critical end point we wish to check the predictions made in I for the behavior of the phase boundary $D_\sigma(T,h)$ near (T_e,D_e).

III. PHASE DIAGRAMS

In this section we present arguments revealing various types of phase diagram that may appear in the model and indicate the corresponding parameter values. We start with a summary of the main conclusions.

A. Overview

Recall first that a tricritical point as illustrated in Fig. 1 is always accompanied by a pair of standard tricritical "wings" when a nonzero ordering field h is introduced: see SF, Fig. 1 and Refs. 11 and 12. However, such a tricritical phase diagram is *never realized when* $d<d_0$ (or $\gamma>2$).[11] Rather, when $d<d_0$ one *always* has an end point and the zero-field phase diagram is as illustrated

schematically in Fig. 2, where E marks the end point while C denotes a new critical point which has classical exponents; see below and Ref. 11. When $h \neq 0$ this critical point extends into a smooth critical line bounding the transition manifold, $D = D_\sigma(T,h)$, that separates the spectator or α phase, at large D, from the ordered $\vec{\beta}_-$ ($m = \pm M_0 > 0$) and disordered β_+ ($m \equiv 0$) phases at low D. Now the critical point C and its extension to nonzero h will not be of direct interest to us beyond their clear association with the presence of the end point E. We observe, however, that when $h = 0$, the associated transition below T_c involves a discontinuity in $m_2 = \langle s^2 \rangle$, although the magnetization $m = \langle s \rangle$ remains zero in the whole vicinity of C. [For $h \neq 0$, of course, m is always nonzero, and there will be an induced jump in m across $D_\sigma(T,h)$.]

For $d \geq d_0$ it transpires that the simple tricritical phase diagram of Fig. 1 may always be found, but appears only if the coefficient p in (2.13), which sets the scale of the variation of $I_d(\zeta)$, is not too large. To be more precise, it is helpful to highlight the dimensionality $d_0 = 3\sigma/2$ at which $\gamma = 2$ by writing

$$(d - d_0)/\sigma = \gamma^{-1} - \tfrac{1}{2} = \epsilon \ . \tag{3.1}$$

Then we define the reduced, dimensionless p coefficient via

$$\bar{p} = \tfrac{1}{2}(1 - 4\epsilon^2) \left[\frac{U^2}{V} \right]^{1/2} p \left[\frac{p}{q} \right]^{2\epsilon/(1-2\epsilon)} , \tag{3.2}$$

noting that

$$\begin{aligned} &\tfrac{1}{2}(1 - 4\epsilon^2) = 2(\gamma - 1)/\gamma^2 \ , \\ &2\epsilon/(1 - 2\epsilon) = (2 - \gamma)/2(\gamma - 1) \ . \end{aligned} \tag{3.3}$$

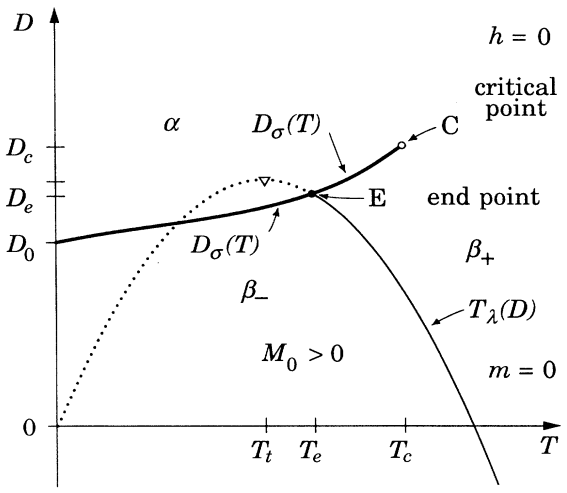

FIG. 2. Zero-field phase diagram displaying an end point on the λ line and a critical point C, with classical exponents. The first-order phase boundary $D_\sigma(T)$ now separates the new α phase from the ordered and disordered phases β_- and β_+. The regimes of dimensionality and Hamiltonian parameters in which this diagram applies are shown in Fig. 3.

When $\epsilon = 0$, $d = d_0$, and $\gamma = 2$, one sees that $\bar{p}$ becomes independent of the correction coefficient q, and, in fact, reduces to the parameter $\dot{p}$ defined by SF. Furthermore, the factors $\sin(\pi/\gamma)$ and $(\gamma - 1)$ in (2.15) and (2.16) conspire with those in (3.2), so that $\bar{p}$ remains well defined in the limit $d \to d_+ -$, $\gamma \to 1+$. One can easily see from (2.15) and (2.16) that the overall magnitude of $\bar{p}$ is set by the dimensionless combination $(U^2/V\hat{J}_\sigma)^{1/2}$. In addition, if one adopts the scaled Kac form, SF (3.7), for $J(\mathbf{R})$ with range R_0 and strength J_0, one finds that $\bar{p}^2$ varies as[15] $(U^2/VJ_0)(a/R_0)^\sigma$. Long-range forces thus lead to small $\bar{p}$.

Now one can report that the simple tricritical phase diagram of Fig. 1 applies whenever $\bar{p} < 1$ and $d \geq d_0$. Beyond that, tricriticality is always realized (for $d \geq d_0$) when

$$\bar{p} < \bar{p}_0(d) = 1 + 2\epsilon \ln \epsilon^{-1} + c_0 \epsilon + \cdots \ , \tag{3.4}$$

where c_0 is a positive coefficient of order unity that is discussed below. More generally, we expect $\bar{p}_0(d)$ to be an increasing function of d: see Fig. 3. It remains finite as $d \to d_+ -$ and, indeed, can be extended to $d > d_+$, where it plays the same role: we discuss this in paper III.[13]

Conversely, whenever $\bar{p}$ exceeds $\bar{p}_0(d)$ and $d \geq d_0$, a critical end point arises (see Fig. 3) and the phase diagram of Fig. 2 applies. This result apparently disagrees with the statement of Ref. 11 (p. 355) that only tricriticality should occur for $d > 3$ ($= d_0$). Note also that Figs. 6 and 7 of Ref. 11 are misleading since they suggest that the critical line which passes through C (called R in Ref. 11) displays a kink at $h = 0$ in the full (T,D,h) space rather than remaining completely smooth as h changes sign.

As stated, tricriticality exists *on* the borderline $d = d_0$

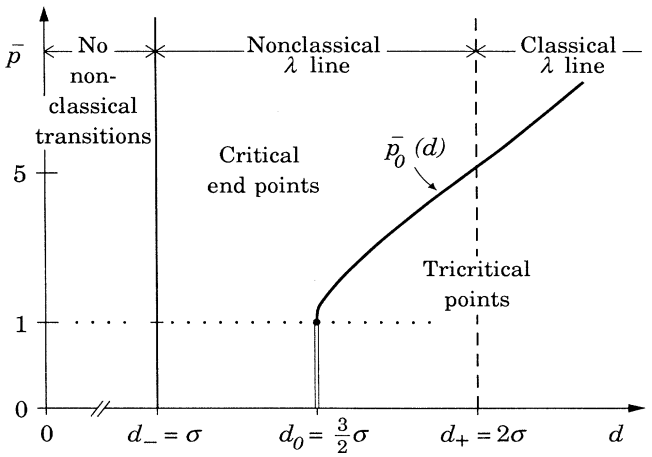

FIG. 3. Schematic depiction of the regimes of tricriticality and critical end points in the plane of dimensionality d and the parameter $\bar{p} \sim (U^2/VJ_0)(a/R_0)^\sigma$, defined explicitly in (3.2). The phase diagram of Fig. 2 applies below $d = d_0$ and above $\bar{p} = \bar{p}_0(d)$. The simple tricritical phase diagram of Fig. 1 applies for $d \geq d_0$ and $\bar{p} < 1$. When $d > d_0$ and $\bar{p}_0 > \bar{p} > 1$, more complex tricritical phase diagrams appear: see subsequent figures. The λ-line exponents are nonclassical for $d_- < d < d_+$ but classical for $d > d_+$. Certain purely classical transitions can occur below d_-: see Ref. 11.

for $\bar{p} < 1$, although it exhibits nonuniversal scaling features (as studied in detail by Sarbach and Fisher).[9,10] The situation is different, however, on the borderline $\bar{p} = \bar{p}_0(d)$ for $d > d_0$. Rather, as illustrated in Fig. 4, this is a limiting case in which the end point *coincides* with the tricritical point, while the critical point C remains distinct at $T_c > T_t$ and $D_c > D_t$. If now d is reduced to d_0 along $p = \bar{p}_0(d)$, the critical point approaches the tricritical end point and all three merge at $d = d_0$. The same happens *at* $d = d_0$ if $\bar{p} > 1$ is reduced to unity. Evidently the point $d = d_0$, $\bar{p} = 1$ represents a special type of multicritical point which might merit further investigation in its own right; however, we have not pursued that task.

On the other hand, if at *fixed* $d > d_0$ the parameter $\bar{p}$ is lowered below $\bar{p}_0(d)$, the tricritical point emerges progressively "from under" the α phase boundary and, as illustrated in Fig. 5, a multiple point Q appears in the $(T,D,h=0)$ plane beneath (T_t,D_t). In the full (T,D,h) space this new point Q is actually a *quadruple* point at which four distinct phases meet, two magnetically ordered with $m = \pm M_0$, and two magnetically disordered with $m \equiv 0$; in the $n=1$ analog one could have coexistence of the four phases α, β, and γ, *and* $\beta\gamma$ at Q. As p falls, the critical point C also moves to lower temperatures and passes "over" the tricritical point, so that, as shown in Fig. 5, $D_c > D_t$. One finds that $T_c = T_t$ on a locus $\bar{p}_1(d)$ having the same form as (3.4) for small ϵ, except that the coefficient c_0 is replaced by $c_1 < c_0$.

On further reduction of p the critical point moves around the tricritical point to lower values of D_c, as shown in Fig. 6: the condition $D_c = D_t$ (with $T_c < T_t$) is attained on a locus $\bar{p}_2(d)$, which again has the form (3.4), but with a coefficient $c_2 < c_1$. Finally, at some $\bar{p}_3(d) > 1$ the critical point C *merges* with the quadruple point Q and disappears into the boundary $D_\sigma(T,h)$ of the β_- phase; the phase diagram then reverts to the simple tricritical form of Fig. 1. The locus $\bar{p}_3(d)$ for small ϵ once more has the form of (3.4) but with a new coefficient $c_3 < c_2$.

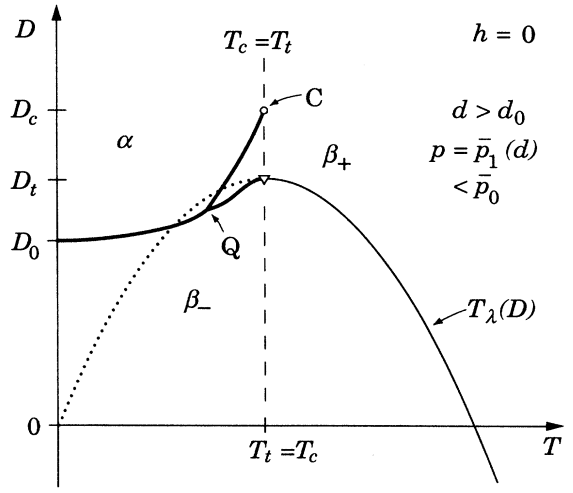

FIG. 5. A more complex tricritical phase diagram than Fig. 1, arising when $d > d_0$ and $\bar{p} > 1$, and including a quadruple point Q and a (classical) critical point C in the special situation when $T_c = T_t$, which occurs when $\bar{p} = \bar{p}_1(d) < \bar{p}_0(d)$.

In the remainder of this section we explain the arguments leading to the conclusions summarized above and embodied in Figs. 1–6. Apart from noticing some new notation and a few corresponding basic expressions for the free energy, etc. that are introduced in the next subsection, a reader uninterested in the details may proceed to Sec. IV.

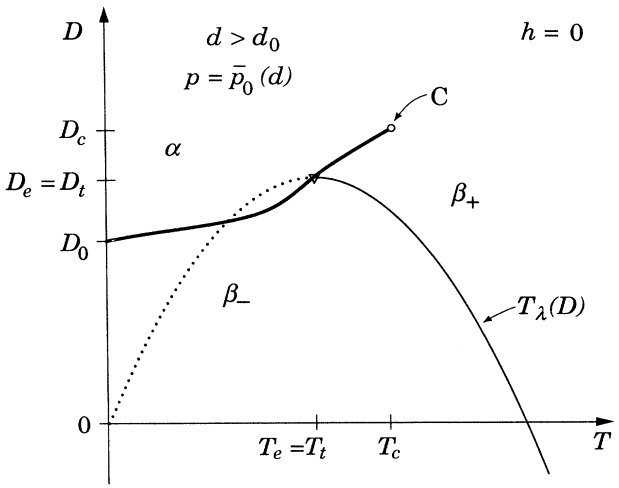

FIG. 4. Phase diagram for $h=0$ and $d > d_0$ in the marginal case $\bar{p} = \bar{p}_0(d)$ in which the critical end point and tricritical point coincide.

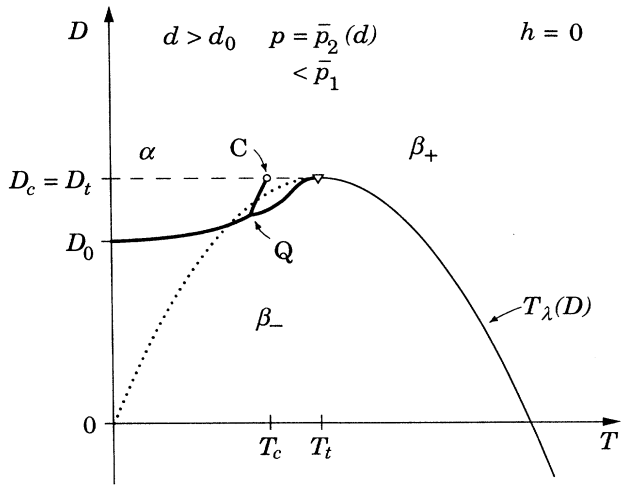

FIG. 6. A complex tricritical phase diagram for $d > d_0$, $\bar{p} > 1$, as in Fig. 5, but meeting the condition $D_c = D_t$, arising when $\bar{p} = \bar{p}_2(d) < \bar{p}_1(d)$.

B. Tricritical vicinity

It is evident from the descriptions of the phase diagrams that the existence of a critical end point hinges on the presence or absence of a tricritical point. The tricritical point, if realized, must have the parameters given in (2.19), together with $\zeta=0$, since it lies on the λ line. Now if there is another value of ζ (and hence of m_2), say, $\zeta_\alpha>0$, which yields a *lower* free energy at the *tricritical location* $(T,D,h)=(T_t,D_t,0)$, then the tricritical point cannot be realized; rather, the "tricritical vicinity" near $(T_t,D_t,0)$ will be occupied by a new phase α. Then, as in Fig. 2, there must be a critical end point on the λ line $T_\lambda(D)$ at a point $(T_e>T_t,\ D_e<D_t)$ where the free energy of the α phase matches that of the critical phase with $\zeta=h=m=0$. Accordingly, it is appropriate to focus attention on the tricritical vicinity. To that end we define

$$t=\frac{T-T_t}{T_t} \quad \text{and} \quad \bar{g}=\frac{D-D_t}{V} \ . \tag{3.5}$$

Later we will define end point deviations $\hat{t}$ and $\hat{g}$. Likewise, in defining the free energy it is useful to make the substitution

$$m_2=\tilde{m}+k_B T I_d^0=\tilde{m}+w(1+t) \ . \tag{3.6}$$

It proves convenient and is adequate for our subsequent purposes to adopt the expansion of $I_d(\zeta)$ in (2.13) as if it were an equality, provided one remembers that the term with p must always dominate that with q. The *constraint equation* (2.8) then becomes

$$\tilde{m}=w(1+t)(-p\zeta^{1/\gamma}+q\zeta)+m^2 \ . \tag{3.7}$$

It follows that $\tilde{m}$ vanishes on the λ line (where $\zeta=m=0$). Likewise, the *minimization equation* (2.9) becomes

$$\zeta/V=\tilde{m}^2+2wt\tilde{m}+\bar{g}+w^2t^2 \ . \tag{3.8}$$

The free energy can be written as the sum of an analytic piece

$$F_0(T,D)=\tfrac{1}{2}k_B T\mathcal{I}_d(\zeta=0;T)+\tfrac{1}{2}D\tilde{T}+\tfrac{1}{4}U\tilde{T}^2+\tfrac{1}{6}V\tilde{T}^3 \ , \tag{3.9}$$

where $\tilde{T}=w(T/T_t)$, which will not concern us further, and a potentially singular part

$$\Delta F(t,\bar{g},h)=w(1+t)[\tfrac{1}{2}(1+\gamma)^{-1}p\zeta^{1+(1/\gamma)}-\tfrac{1}{4}q\zeta^2]+\tfrac{1}{6}\tilde{m}^3V+\tfrac{1}{2}[wt\tilde{m}^2+(\bar{g}+w^2t^2)\tilde{m}]V-hm \ , \tag{3.10}$$

which also vanishes identically on the λ line and its parabolic extension. Note that the assignment

$$U=-2, \quad V=1 \tag{3.11}$$

corresponds only to a specific choice of units for energy, spin, and field and yields $w=1$ and $D_t=1$; it thus simplifies the appearance of (3.6)–(3.9) and will be adopted below when convenient.

C. Tricriticality criterion

If we specialize to the tricritical location $t=\bar{g}=h=0$ and eliminate $\tilde{m}$ between the constraint and minimization equations we find the equation

$$\zeta=w^2V(p\zeta^{1/\gamma}-q\zeta)^2 \ , \tag{3.12}$$

while the free energy reduces to

$$\Delta F_t(\zeta)=-\tfrac{1}{12}w\left[\frac{-8\epsilon}{3+2\epsilon}p\zeta^{\epsilon}+q\zeta^{1/2}\right]\zeta^{3/2} \ . \tag{3.13}$$

Evidently (3.12) has a solution $\zeta=0$, yielding $\Delta F_t=0$, that corresponds just to the tricritical point. If we cancel this solution, take the square root, rescale by putting $\zeta=\bar{\zeta}(p/q)^{2/(1-2\epsilon)}$, and recall (3.1) and (3.2), we obtain the *tricriticality equation*[16]

$$(1-4\epsilon^2)/\bar{p}=\bar{\zeta}^{\epsilon}-\bar{\zeta}^{1/2} \quad (\zeta>0) \ . \tag{3.14}$$

Consider first the case (i) $\epsilon=0$ (or $d=d_0$ with $\gamma=2$). There are clearly no solutions unless $\bar{p}>1$. Consequently, if $\bar{p}<1$ we conclude that a tricritical point (with $\zeta=0$) must be realized, so confirming the conclusion stated above in Sec. III A. Conversely, for $\bar{p}>1$ there is always a solution $\zeta_\alpha>0$; furthermore, by (3.13), we see that $\Delta F_t(\zeta_\alpha)$ is then negative. We conclude that a critical end point with a phase diagram like Fig. 2 must occur for $d=d_0$ when $\bar{p}>1$. Of course, $\bar{p}=1$ is a special situation; in fact, as remarked before, the end point, the tricritical point, and the new critical point C all then coincide.

Next consider (ii) the case $\epsilon<0$ (or $d<d_0$ and $\gamma>2$). The right side of (3.14) now decreases monotonically from $+\infty$ as ζ increases from zero and scans all positive values.[16] Evidently there is a solution $\zeta_\alpha>0$ for *all* $\bar{p}>0$. Again, by (3.13) the free energy is always lowered. We thus confirm the conclusion[11] that *only* critical end points appear for $d<d_0$.

The last case (iii) $\epsilon>0$ (or $d>d_0$ and $\gamma<2$) is the most interesting. Note, in the first place, that the two terms in (3.13) now compete. Secondly, the right side of (3.14) now has a maximum at $\bar{\zeta}_m=(2\epsilon)^{2/(1-2\epsilon)}$. From that we see that there can be no solutions if $\bar{p}<\bar{p}_m(d)$, where

$$\bar{p}_m(d)=(2\epsilon)^{-2\epsilon/(1-2\epsilon)}(1+2\epsilon) \ , \tag{3.15}$$

which has an expansion of the form (3.4) but with $c_m=2(1-\ln 2)\simeq 0.6137$.

Tricriticality is thus ensured for $\bar{p}<\bar{p}_m$. However, although there are solutions for ζ, suggesting an end point, whenever $\bar{p}>\bar{p}_m$, one finds $\Delta F_t>0$ for $\bar{p}\gtrsim\bar{p}_m$, so they are not all stable. As ζ increases above ζ_m, however, ΔF_t decreases monotonically. The true borderline between the tricritical and end point regimes can thus be found by eliminating ζ between (3.14) and the equation $\Delta F_t=0$. This yields

$$\zeta_0(d)=\left[\frac{8\epsilon}{3+2\epsilon}\frac{p}{q}\right]^{2/(1-2\epsilon)} \tag{3.16}$$

and then

$$\bar{p}_0(d)=\left[\frac{8\epsilon}{3+2\epsilon}\right]^{-2\epsilon/(1-2\epsilon)}(1+2\epsilon)(1+\tfrac{2}{3}\epsilon)\ , \quad (3.17)$$

which has the expansion (3.4) with

$$c_0=\tfrac{8}{3}-2\ln\tfrac{8}{3}\simeq 0.7050>c_m\ . \quad (3.18)$$

For solutions of (3.14) with $\zeta_\alpha>\zeta_0$ the new α phase always has a lower free energy at the tricritical location and, hence, an end point is always present, and Fig. 2 applies. Clearly, the borderline $\bar{p}=\bar{p}_0$ with two solutions $\zeta=0$ and ζ_α, having equal free energies, corresponds to Fig. 4.

It should be remarked that although written as equalities, the above expressions for $\zeta_0(d)$ and $\bar{p}_0(d)$ rely on truncating the expansion (2.13) for $I_d(\zeta)$. They are thus quantitatively valid only for $\bar{\zeta}\ll 1$ or, more concretely, when $2\epsilon^2\ll 1$.

To complete the elucidation of the phase diagrams for $p\lesssim\bar{p}_0(d)$ we turn to the task of locating the new critical point C. The discussion of the end point vicinity is taken up again in Sec. IV.

D. Classical criticality

In order to complete the justification of Figs. 4, 5, and 6 and to determine the appropriate values of $\bar{p}$, we study the location of the critical point C in zero field. Since this occurs away from $\zeta=0$ we expect, as mentioned, purely classical behavior. Accordingly, we seek values of t and $\bar{g}$ at which the solutions for ζ and $\tilde{m}$, which are related through the constraint and minimization equations (3.7) and (3.8), *bifurcate,* one root splitting into three, say ζ^+, ζ^0, and ζ^-, in the usual phenomenological or van der Waalsian manner. The confluence of the three roots locates the critical point. Thus, if we write (3.7) and (3.8) as

$$\tilde{m}=u^{-1}(\zeta)\ \text{ and }\ \zeta=v(\tilde{m})=\tilde{m}^2+2t\tilde{m}+\bar{g}+t^2\ , \quad (3.19)$$

where for brevity we have used (3.11), the conditions for criticality are simply

$$u(\tilde{m})=v(\tilde{m}),\quad u'(\tilde{m})=v'(\tilde{m})=2\tilde{m}+2t\ , \quad (3.20)$$

$$u''(\tilde{m})=v''(\tilde{m})=2\ . \quad (3.21)$$

To analyze these equations we put

$$\zeta=u=(pz/q\gamma)^{2/(1-2\epsilon)}\ , \quad (3.22)$$

and express u'' in terms of u', and then in terms of z alone. Then (3.21) yields the *criticality equation*

$$\bar{p}^{\,2}(1-z)^3=K(z/\gamma)^{-4\epsilon/(1-2\epsilon)}\ , \quad (3.23)$$

where $K=(1-2\epsilon)^3/(1+t)^2$. This is readily understood graphically. For (i) $\epsilon=0$ there are solutions only for $(1+t)\bar{p}\geq 1$ and one then has $z\approx\frac{2}{3}(\Delta\bar{p}+t)$ for small $\Delta\bar{p}=\bar{p}-1$ and t. The restriction, in fact, corresponds to the existence of an end point and associated critical point only for $\bar{p}>1$, as previously observed: see Fig. 3.

When one has (ii) $\epsilon<0$ there are always solutions, which vary as

$$z\approx\gamma[(1+t)\bar{p}/(1-2\epsilon)^{3/2}]^{(1-2\epsilon)/2|\epsilon|} \quad (3.24)$$

for small $\bar{p}$. The divergence of the exponent as $\epsilon\to 0-$ is indicative of the fact that tricriticality takes over at small $\bar{p}$ when $\epsilon=0$: see Fig. 3. Finally, for (iii) $\epsilon>0$ there are no solutions if $\bar{p}$ is small, but two solutions arise for $\bar{p}$ large enough.

Now, given a solution z (and hence ζ_c) we can use (3.19) for $\tilde{m}$ and solve the second member of (3.20) to find the critical value t_c. Then one can return to $v(\tilde{m})$ in (3.19) to find $\bar{g}_c$. The algebra is involved, but finally yields

$$t_c=\frac{\sqrt{V}}{|U|}\left[\frac{pz}{q\gamma}\right]^{1/(1-2\epsilon)}\frac{\frac{1}{2}\gamma+z'-2z'^2}{(z')^{3/2}}\ , \quad (3.25)$$

$$\bar{g}_c=\frac{1}{V}\left[\frac{pz}{q\gamma}\right]^{2/(1-2\epsilon)}(1-z')\ , \quad (3.26)$$

where we have restored the factors of U and V and put

$$z'=(1-z)/(1-2\epsilon)\ . \quad (3.27)$$

One should recall that z depends on t so that these relations are not fully explicit; however, the dependence on t is weak and turns out not to enter in leading orders near $\epsilon=0$ and $\bar{p}=1$.

We will not analyze these equations fully, but a few limits are especially instructive. When $\epsilon=0$ ($d=d_0$) and $\Delta\bar{p}=\bar{p}-1>0$ is small one finds $t_c\approx j_0\Delta\bar{p}^{\,2}$, $\bar{g}_c\approx k_0\Delta\bar{p}^{\,3}$, and $z\sim\Delta\bar{p}$ with $j_0,k_0>0$. This confirms that C approaches the tricritical point when $\bar{p}\to 1+$.

Figure 5 illustrates the special case in which $T_c=T_t$ or $t_c=0$. By (3.25) this condition yields the locus

$$\bar{p}=\bar{p}_1(d)\approx\left[\tfrac{4}{3}\epsilon\right]^{-2\epsilon}(1+\epsilon+\cdots) \quad (3.28)$$

for ϵ small but positive; this has the form (3.4) with $c_1=1-2\ln\frac{4}{3}\simeq 0.4246<c_0$. On this locus one also has $z\sim\epsilon$ and $\bar{g}_c\approx k_1\epsilon^2$ with $k_1>0$.

In Fig. 6 the critical point has moved below T_t and met the special condition $D_c=D_t$ or $\bar{g}_c=0$. From (3.25) and (3.26) we find $z\sim\epsilon$ and $t_c\approx -j_2\epsilon^2$ with $j_2>0$ and

$$\bar{p}=\bar{p}_2(d)\approx(\epsilon)^{-2\epsilon}[1+O(\epsilon^2)]\ , \quad (3.29)$$

which again has the form (3.4) but with $c_2=0$.

Finally, we may use the results for z, t_c, and $\bar{g}_c$ to evaluate the free energy at the α-β_+ critical point in terms of z. If this is matched to the free energy of the ordered phase $\vec{\beta}_-$, which follows by setting $\zeta\equiv 0$, one obtains an equation for the locus $\bar{p}_3(d)$ on which C merges with the quadruple point Q: see Figs. 5 and 6. This yields

$$\bar{p}_3(d)\approx(\tfrac{8}{9}\epsilon)^{-2\epsilon}(1-\tfrac{1}{3}\epsilon+\cdots)\ , \quad (3.30)$$

which once more follows (3.4) but with $c_3=2\ln\frac{9}{8}-\frac{1}{3}\simeq -0.0978$. Note that even though $c_3<0$, the locus $\bar{p}_3(d)$ lies above $\bar{p}=1$ for small ϵ and is expected to do so generally. At least for ϵ relatively small, the merging of C and Q occurs away from $T=0$ and, in fact, rather close to T_t.

The quadruple point in Figs. 5 and 6 lies inside the parabola corresponding to the extended λ line (shown as a dotted line). This is established by showing that the β_+-β_- phase boundary $D_\sigma(T)$ near the tricritical point lies inside the parabola for $\bar{p} > 1 + c_4\epsilon$ with $c_4 > 0$. For $\bar{p} \leq 1$, however, $D_\sigma(T)$ lies wholly outside the λ parabola, as shown in Fig. 1.

This completes our discussion of the phase diagrams. We focus next on the λ line in order to understand the end point region.

IV. FREE ENERGY NEAR THE LAMBDA LINE

Having established the circumstances in which a critical end point will exist, we wish to study the phase boundaries in its vicinity in greater detail. To that end we obtain, in this section, the behavior of the free energy of the β_+ and β_- phases in the vicinity of the λ line $T_\lambda(D)$. In the following section, the free energy of the disordered α phase will be discussed; that will put us in a position to determine the phase boundary $D_\sigma(T,h)$ and to check the predictions outlined in the Introduction.

It is convenient to measure the deviation from the critical line λ in the (T,D) plane in terms of

$$\tilde{t} = \bar{g} + w^2 t^2 , \tag{4.1}$$

which vanishes *on* λ. Now ζ vanishes on (and below) λ. Thus we organize the free energy (3.10) and the associated constraint and minimization relations (3.7) and (3.8) in powers of ζ. By combining (3.8) and (3.10), and neglecting the additive analytic piece (3.9), the free energy becomes

$$\Delta F = \frac{wp(1+t)}{2(1+\gamma)}\zeta^{(\gamma+1)/\gamma}[1+O(\zeta^{(\gamma-1)/\gamma})] - hm - \frac{1}{8}\frac{V}{wt}\tilde{t}^2 - \frac{1}{6}\frac{V}{(2wt)^3}\tilde{t}^3 + O(\tilde{t}^4) . \tag{4.2}$$

Consider first the case $h \to 0$ whence $\zeta = \chi^{-1}$. With the aid of (3.7) we find the susceptibility diverges as

$$\chi = \zeta^{-1} \approx C_+ / \tilde{t}^\gamma [1 + O(\tilde{t}^{\gamma-1}, \tilde{t})] , \tag{4.3}$$

when $\tilde{t} \to 0+$ [above $T_\lambda(D)$], where the amplitude is

$$C_+ = [2w^2 pt(1+t)]^\gamma . \tag{4.4}$$

The singular part of the β-phase free energy in a small field then follows from (4.2) and can be written as

$$\Delta F^s_{\beta+} = -\frac{A_+}{(2-\alpha)(1-\alpha)}\tilde{t}^{2-\alpha}[1 + O(\tilde{t}^{\gamma-1}, \tilde{t})] + \tfrac{1}{2}C_+ \tilde{t}^{-\gamma} h^2 [1 + O(\tilde{t}^{\gamma-1}, \tilde{t}, h^2/t^{2\Delta})] \tag{4.5}$$

($\tilde{t} > 0$) where the specific-heat amplitude is

$$A_+ = -\tfrac{1}{2}\gamma wp(1+t)/[2w^2 pt(1+t)]^{\gamma+1} . \tag{4.6}$$

In zero field below $T_\lambda(D)$ one has $\zeta = \chi^{-1} = 0$, so that there are only analytic terms in the free energy; thus, as is well known, one has $A_- = 0$, while C_- is undefined. On the other hand, $\tilde{m} = m^2$ is nonzero, and the spontaneous magnetization follows from (3.8) as

$$m_0 \approx B|\tilde{t}|^\beta [1 + O(\tilde{t})] , \tag{4.7}$$

with exponent and amplitude

$$\beta = \tfrac{1}{2}, \quad B = 1/(2wt)^{1/2} . \tag{4.8}$$

Further, when $h \to 0$, one finds $m - m_0 \sim |h|^{1/\gamma}/|\tilde{t}|^{(\gamma+1)/2\gamma}$. In a small field beneath T_λ the singular part of the β-phase free energy is thus

$$\Delta F^s_{\beta-} = -B|\tilde{t}|^\beta |h| [1 + O(|h|^{1/\gamma}/|\tilde{t}|^{\delta/2\gamma})] . \tag{4.9}$$

Finally, on the critical isotherm ($\tilde{t} = 0$) one readily finds

$$m \approx B_c |h|^{1/\delta} \quad \text{and} \quad \Delta F^s_{\beta c} \approx -\frac{B_c \delta}{\delta+1}|h|^{(\delta+1)/\delta} , \tag{4.10}$$

with exponent $\delta = 2\gamma + 1$ and amplitude

$$B_c = [wp(1+t)]^{\gamma/(2\gamma+1)} . \tag{4.11}$$

The universal amplitude ratios (see I) follow as $A_-/A_+ = 0$ and

$$\Theta_1 = \frac{A_+ C_+}{B^2} = -\tfrac{1}{2}\gamma, \quad \Theta_2 = \frac{A_+ B_c^\delta}{B^{\delta+1}} = -\tfrac{1}{2}\gamma , \tag{4.12}$$

so that $\Theta_3 = B^{\delta-1} C_+ / B_c^\delta = 1$ and $\Theta_4 = A_+^{\delta-1} C_+^{\delta+1} / B_c^{2\delta} = (\frac{1}{2}\gamma)^{2\gamma}$. It might be remarked that when $1 - \alpha = \gamma$ is an integer, the singular part of the free energy above T_λ varies as an integral power of $\tilde{t}$, and so cannot be obviously separated from the analytical background. However, it is clear by continuity in σ (or d) and by the association with $\zeta(T)$ that the assignment $A_- = 0$ is appropriate.

V. CRITICAL END POINT AND THE SPECTATOR PHASE

It is fairly clear from our discussion of the spectator phase α in Sec. III that the spherical field ζ never vanishes in this phase. In particular, at the end point itself, one has $\zeta_{\alpha,e} > 0$; by continuity, the same must hold in the vicinity of the end point E (even if E resides *at* the tricritical location, as illustrated in Fig. 4). Furthermore, the classical critical point C is separated from E (provided it does not lie *at* the tricritical location, as can happen only when $d = d_0$ and $\bar{p} = 1$). Consequently, the α-phase free energy will be an analytic function of $\hat{t}$, $\hat{g} = \bar{g} - \bar{g}_e$, and h, the deviations from the end point. This will be true wherever the α-phase free energy is defined and, in particular, will hold *on* (and some way beyond) the α-β phase boundary $D_\sigma(T,h)$. Since the β-phase free energy is also well defined everywhere near the λ-line parabola by (4.5), (4.9), and (4.10), etc., the boundary itself may be obtained by equating free energies. But this is just the situation that was envisaged phenomenologically in I. The general conclusions of I regarding the singularities in the α-β phase boundary must, therefore, follow here also, provided only that proper allowance is made for the special features of the spherical model.

While these arguments serve formally to complete the verification of I as regards our general spherical models, it is instructive to exhibit the parameters of the end point and the nature of the α-phase free energy somewhat more explicitly. Accordingly, let us return to (3.7) and (3.8),

the constraint and minimization equations, and recall the definition (4.1) of $\tilde{t}$. On taking the product of (3.7) and (3.8) and reusing (3.8) one can eliminate ζ from the free-energy expression (3.10) to obtain, without further approximation,

$$\Delta F(t,\bar{g},h) = -hm + V\sum_{j=0}^{4}[K_j(\tilde{t})+L_j(\tilde{t})m^2]\tilde{m}^j , \quad (5.1)$$

where $K_j(\tilde{t})$ and $L_j(\tilde{t})$ are quadratic polynomials given by

$$K_0 = k_0''\tilde{t}^2,\quad K_1 = k_1'\tilde{t},\quad K_2 = k_2 + k_2'\tilde{t} , \quad (5.2)$$
$$K_3 = k_3,\quad K_4 = k_4 ,$$

$$L_0 = l_0'\tilde{t},\quad L_1 = l_1,\quad L_2 = l_2,\quad L_3 \equiv L_4 \equiv 0 , \quad (5.3)$$

with coefficients depending only on t. If, for brevity, we put

$$w' = w(1+t),\quad \gamma_+ = \gamma+1,\quad \Gamma = \frac{\gamma-1}{\gamma+1} , \quad (5.4)$$

we have, explicitly,

$$k_0'' = -\tfrac{1}{4}V\Gamma w' q,\quad k_1' = \tfrac{1}{2}\gamma/\gamma_+ - V\Gamma w' w q t , \quad (5.5)$$

$$k_2 = \tfrac{1}{2}\Gamma(1-2Vw'wqt)wt,\quad k_2' = -\tfrac{1}{2}V\Gamma w' q , \quad (5.6)$$

$$k_3 = \tfrac{1}{6}(\gamma-2)/\gamma_+ - V\Gamma w' w q t,\quad k_4 = -\tfrac{1}{4}V\Gamma w' q , \quad (5.7)$$

$$l_0' = l_2 = 1/2\gamma_+,\quad l_1 = wt/\gamma_+ . \quad (5.8)$$

Now, in principle, (3.7) and (3.8) may be solved to yield $\tilde{m}(t,\bar{g},h)$; then $\zeta(t,\bar{g},h)$ follows directly from (3.8). On the λ line $\tilde{t} = \bar{g} + w^2 t^2$ vanishes identically as do m, h, and $\tilde{m}_\beta$ and ζ_β. The α phase, however, is specified by a root $\tilde{m}_\alpha(t,\bar{g},h)$ that does *not* vanish when $\tilde{t}\to 0$ (with $h=0$). On the other hand, at the end point itself we have $\Delta F_\alpha = \Delta F_\beta = 0$, by continuity of the free energy. Equating (5.1) to zero on λ ($\tilde{t}=h=0$) and canceling the vanishing roots $\tilde{m}_\beta = 0$ yields the quadratic equation

$$\tilde{m}_{\alpha e}^2 - b(t_e)\tilde{m}_{\alpha e} + c(t_e) = 0 , \quad (5.9)$$

for $\tilde{m}_{\alpha e} \equiv \tilde{m}_\alpha(t_e,\bar{g}_e,0)$, the end-point value of $\tilde{m}_\alpha$. The coefficients follow from (5.6) and (5.7) as

$$b = \tfrac{2}{3}(\gamma-2)/(\gamma-1)Vw'q - 4wt , \quad (5.10)$$

$$c = -2t/Vq(1+t) + 4w^2t^2 . \quad (5.11)$$

The end-point equation (5.9) can now be solved in conjunction with (3.7) and (3.8) to yield the end-point parameters t_e, $\tilde{m}_{\alpha e}$, and $\zeta_{\alpha e}$. (Of course, $\bar{g}_e = -w^2 t_e^2$ follows from $\tilde{t}=0$.) The analysis must be performed separately in the regimes $d \gtrless d_0$ and is only tractable when t_e is small; however, that is really the only situation of true concern. We quote some results as follows: first (a) for $d < d_0$ or $\gamma > 2$,

$$t_e \approx \frac{1}{3}\frac{\gamma-2}{\gamma-1}\left[\frac{\gamma+1}{\gamma-1}\frac{Vw^2}{3}\right]^{1/\gamma-2} p^{\gamma/(\gamma-2)} , \quad (5.12)$$

$$\tilde{m}_{\alpha e} \approx -3\frac{\gamma-1}{\gamma-2}wt_e,\quad \zeta_{\alpha e} \approx 3V\frac{\gamma^2-1}{(\gamma-2)^2}w^2t_e^2 . \quad (5.13)$$

These expressions neglect correct factors $[1+O(q)]$ with coefficients diverging as $\gamma\to 2-$. Note that the exponents also diverge in this limit; that is indicative of the behavior of the tricritical–end-point boundary at $d \simeq d_0$, illustrated in Fig. 3. As indicated, corrections of order t_e itself also arise; basically, this means that p must not be too large if (5.12) is to remain valid.

Next, (b) on the borderline $d = d_0$ or $\gamma = 2$ one finds (with some care)

$$t_e \approx \tfrac{2}{9}(\bar{p}-1)^2/Vw^2q , \quad (5.14)$$

$$\tilde{m}_{\alpha e} \approx -\frac{2}{3}\frac{\bar{p}-1}{Vwq},\quad \zeta_{\alpha e} \approx \frac{4}{9}\frac{(\bar{p}-1)^2}{Vw^2q^2} , \quad (5.15)$$

subject to corrections of relative order $\bar{p}-1$ where $\bar{p} = \sqrt{V}wp$ [see (3.2)]. Recall from Sec. III and Fig. 3 that a critical end point exists when $d = d_0$ *only if* $\bar{p} > 1$.

Finally, (c) for $d > d_0$ or $\gamma < 2$ we recall, again from Fig. 3, that a critical end point occurs *only if* $\bar{p} > \bar{p}_0(d)$, given, for small $\epsilon = (d-d_0)/\sigma$, by (3.4) with (3.18). When $\bar{p} - \bar{p}_0(d)$ is positive but small, t_e is also small: compare Figs. 4 and 2. In these circumstances one obtains directly from (5.9), and then from (3.8),

$$\tilde{m}_{\alpha e} \approx -\tfrac{2}{3}\left[\frac{2-\gamma}{\gamma-1}\right]\frac{1}{Vwq},\quad \zeta_{\alpha e} \approx \tfrac{4}{9}\left[\frac{\gamma-2}{\gamma-1}\right]^2\frac{1}{Vw^2q^2} , \quad (5.16)$$

subject to corrections of relative order t_e. However, it is not easy to give a general expression for t_e itself. When $\bar{p} - \bar{p}_0$ and ϵ are both small, one can, nevertheless, derive the expression

$$t_e = \tfrac{32}{27}(\bar{p}-\bar{p}_0)\frac{\epsilon}{Vw^2q}(\tfrac{8}{3}\epsilon)^{4\epsilon} . \quad (5.17)$$

Once the end-point parameters are determined, it is straightforward but tedious to return to (3.7) and (3.8) to obtain convergent Taylor-series expansions for $\tilde{m}_\alpha$ and m_α in powers of $\hat{t} = t - t_e$, $\hat{g} = \bar{g} - \bar{g}_e$ (or, more conveniently, in $\tilde{t} = \bar{g} + w^2t^2$) and h^2. Substitution in (5.1) then yields

$$F_\alpha = F_0(T,D) + \sum_{i,j}(Q_{ij} + h^2R_{ij} + \cdots)\hat{g}^i\hat{t}^j , \quad (5.18)$$

where F_0 is the analytic piece given in (3.9), while the coefficients Q_{ij} and R_{ij} depend only on γ and the parameters V, w, p, and q. In fact, the leading coefficients Q_{ij} have been computed explicitly in the regime (a) above ($d < d_0$, p not too large), but the expressions are lengthy and not very informative. It transpires that to compute the leading singularities in the phase boundary one does *not* need the coefficients R_{ij}. The range of convergence of (5.18) should be determined by the location of the classical critical point C and by the associated spinodal line in the (T,D) plane which marks the intrinsic limit of stability of the α phase.

VI. PHASE BOUNDARY AND AMPLITUDE PREDICTIONS

In (5.18) the free energy of the α phase is represented as a Taylor-series expansion about the end point $(t_e,\bar{g}_e,0)$ in powers of the end-point deviations $\hat{t}$, $\hat{g}$, and h. Expressions for the singular pieces of the free energies of the β_+ and β_- phases for small h close to the end point are given in (4.5) and (4.9). [Note that the *total* free energy F_β is obtained by adding the analytic powers of $\tilde{t}$ contained in (4.2) and the analytic background F_0 from (3.9).] The singular piece $\Delta F^s_{\beta c}$ *on* the λ line is given in (4.10).

As already observed, the phase boundary $D_\sigma(T,h)$, or $\hat{g}_\sigma(\hat{t},h)$, can now be computed near the end point by matching the α and β expressions in the various regimes. The details proceed just as in I and will not be repeated here. For completeness, however, we review the results briefly. First, in small fields, the α-β boundary has the form (1.2), except that below T_e ($\hat{t}<0$) the amplitude X_- vanishes identically. In addition, the amplitude Z_- is not defined, since the field variation beyond the $|h|$ term is now proportional to $|h|^{(\gamma+1)/\gamma}$; this feature is characteristic of an $O(n)$ order parameter with $n>1$. Actually, we could, if we chose, define a corresponding amplitude in $\Delta F^s_{\beta-}$ and D_σ that would also then satisfy an appropriate universality relation.

The nonvanishing amplitudes X_+, Y_-, and Z_+ are simply related to the λ-line amplitudes A_-, B, and C_+ via the coefficients Q_{ij} in (5.18). On forming the ratio X_-/X_+ in accord with the general predictions (1.3) and (1.4), we find the trivial concordance $X_-/X_+=0=A_-/A_+$. Less trivially we obtain

$$\Xi_1\equiv X_+Z_+/Y_-^2=-1/2(\gamma+1)\ . \tag{6.1}$$

In light of (4.12) and the relation $(2-\alpha)(1-\alpha)=\gamma(\gamma+1)$ [see (2.17)] this confirms the prediction (1.4) relating Ξ_1 to $\Theta_1\equiv A_+C_+/B^2$.

As in I, it is also interesting to study the $D_\sigma(T,h)$ surface as a function of h *on* the end-point isotherm $T=T_e$. We obtain

$$D_\sigma(T_e,h)-D_e=-(Y_c/e_0)|h|^{(\delta+1)/\delta}+O(h^2)\ , \tag{6.2}$$

where the geometrical factor [see I (5.4)] is

$$e_0=1-\left[\frac{\partial D_\sigma}{\partial T}\right]_{h=0,e}\left[\frac{dT_\lambda}{dD}\right]_e\ , \tag{6.3}$$

which can be evaluated explicitly in terms of t_e and the coefficients Q_{ij}. The amplitude Y_c is likewise found in terms of B_c [see (4.11)]. We may now check the prediction

$$\Xi_2\equiv\frac{X_+Y_c^\delta}{Y^{\delta+1}}=\frac{\Delta^\delta\Theta_2}{(2-\alpha)^{\delta+1}(1-\alpha)}\ , \tag{6.4}$$

[see I (5.15)] where $\Theta_2=A_+B_c^\delta/B^{\delta+1}$ was evaluated in (4.12) above. One finds for our spherical models

$$\Xi_2=-(2\gamma+1)^{2\gamma+1}/(2\gamma+2)^{2\gamma+2}\ , \tag{6.5}$$

which on using (2.17) is seen to verify the prediction. Likewise, the predictions for Ξ_3 and Ξ_4 in terms of Θ_3 and Θ_4 [see I, (5.16) and (5.17)] may be checked.

In conclusion, we have exhibited a series of nontrivial critical end points in spherical models of general dimensionality with short-range and power-law interactions. The phase boundary between the spectator phase and the critical phases exhibits singularities as the end point is approached [see (1.2) and (6.2)]. The amplitudes of these phase-boundary singularities combine to yield universal dimensionless ratios. These ratios, in turn, are directly related to corresponding universal bulk amplitude ratios evaluated on the λ line that terminates at the end point. The form of these relations obeys the general, phenomenological predictions advanced in I.

In retrospect, our findings are not so surprising. The main effort required is to establish the existence and location of end points in the spherical models. Within the spherical-model theory no mechanism for the production of droplet singularities [see I] was apparent previously and none has appeared here. The $O(n>1)$ or spin wave singularities at the standard spherical-model ferromagnetic phase boundaries affect the form of the spectator phase boundary, but *no* new singularities of any sort appear in the spectator phase itself. The mechanism of α-β phase coexistence turns out to be just the "classical" one of the crossing of two separate (although, of course, ultimately related) branches of the free energy; that is, of course, in accord with the phenomenological theory. It remains conceivable, however, that models displaying end points with criticality described by finite n (as against $n\to\infty$ for spherical models) might violate the predictions of I.

ACKNOWLEDGMENTS

One of us (M.C.B.) is grateful for the hospitality accorded by the Institute for Science and Technology at the University of Maryland and to the Conselho Nacional de Desenvolvimento Cientifico e Technologico (CNPq) for support during the period when most of this research was completed. The National Science Foundation has also provided support (currently under Grant No. DMR 90-7811).

APPENDIX: CRITICAL BEHAVIOR OF $I_d(\zeta)$

The basic correlation integral is given by (2.11) and (2.10) as

$$I_d(\zeta)=\int\frac{a^d d^d k}{(2\pi)^d}\frac{1}{\zeta+\Delta\hat{J}(\mathbf{k})}\ , \tag{A1}$$

where the integral runs over the appropriate Brillouin zone $\mathcal{B}$, which for a hypercubic lattice is specified simply by $-\pi<k_\lambda a\le\pi$ for each component $k_\lambda=(\mathbf{k})_\lambda$ ($\lambda=1,\ldots,d$). Following (2.5) we can write

$$\Delta\hat{J}(\mathbf{k})\equiv\hat{J}(\mathbf{0})-\hat{J}(\mathbf{k})=P|\mathbf{k}a|^\sigma+E(\mathbf{k}a)\ , \tag{A2}$$

where $P\equiv\hat{J}_\sigma$ and $E(\mathbf{y})=o(y^\sigma)$ as $|\mathbf{y}|\to 0$; however, we will need to specify $E(\mathbf{y})$ more closely. Accordingly, we suppose $\Delta\hat{J}(\mathbf{k})$ is finite and bounded away from zero everywhere in $\mathcal{B}$ except near the origin, where

$$E(\mathbf{y})=Q|\mathbf{y}|^2+o(|\mathbf{y}|^2)\ . \tag{A3}$$

One could certainly contemplate more singular terms entering $E(\mathbf{y})$; however, merely by considering changes in the interactions $J(\mathbf{R})$ at short distances, one sees that one cannot, in general, avoid terms of quadratic order.

We desire the behavior of $I_d(\zeta)$ when $\zeta\to 0$ for the range $\sigma<d<2\sigma$: see (2.12). In this case $I_d^0\equiv I_d(\zeta\to 0)$ is well defined and so we can write the identity

$$\Delta I_d\equiv I_d(\zeta)-I_d^0=-\int_{ka}\frac{\zeta}{\Delta\hat{J}(\mathbf{k})[\zeta+\Delta\hat{J}(\mathbf{k})]}$$
$$=G_0(\zeta)+G_2(\zeta)+G_3(\zeta)\ , \tag{A4}$$

where $\int_q$ denotes $(2\pi)^{-d}\int d^dq$ with $|q_\lambda|\le\pi$ (all λ), while

$$G_0(\zeta)=-\int_q\frac{\zeta P^{-1}q^{-\sigma}}{\zeta+Pq^\sigma}\ , \tag{A5}$$

$$G_2(\zeta)=\int_q\frac{\zeta P^{-1}q^{-\sigma}E(\mathbf{q})}{(\zeta+Pq^\sigma)[\zeta+Pq^\sigma+E(\mathbf{q})]}\ , \tag{A6}$$

$$G_3(\zeta)=\int_q\frac{\zeta P^{-1}q^{-\sigma}E(\mathbf{q})}{[Pq^\sigma+E(\mathbf{q})][\zeta+Pq^\sigma+E(\mathbf{q})]}\ . \tag{A7}$$

Now consider $G_1(\zeta)$: add and subtract the integral over $\bar{\mathcal{B}}$, the whole of momentum space *outside* $\mathcal{B}$, and rescale by putting $Pq^\sigma=\zeta y$ to obtain

$$G_0(\zeta)=-\frac{\zeta^{1/\gamma}}{\sigma P^{d/\sigma}}\frac{\Omega_d}{(2\pi)^d}\int_0^\infty\frac{y^{(d-2\sigma)/\sigma}}{1+y}dy+G_1(\zeta)\ , \tag{A8}$$

where $\Omega_d=2\pi^{d/2}/\Gamma(d/2)$, while

$$G_1(\zeta)=\frac{\zeta}{p^2}\frac{\Omega_d}{(2\pi)^d}\int_{\bar\pi}^\infty\frac{dq}{q^{2\sigma-d+1}}\left[1+O\left[\frac{\zeta}{Pq^\sigma}\right]\right] \tag{A9}$$

represents the contribution from $\bar{\mathcal{B}}$. Now a sphere of radius π can be inscribed in $\mathcal{B}$, while a sphere of radius $\pi\sqrt{d}$ circumscribes $\mathcal{B}$. Consequently, a proper choice of $\bar\pi(d,\sigma)$ satisfying $1\le\bar\pi/\pi\le\sqrt{d}$ makes (A9) an identity. Evaluation of the integrals in (A8) and (A9) is simple and leads, if G_2 and G_3 are ignored, to the form (2.13) for $I_d(\zeta)$, with coefficients p and q given precisely by (2.15) and (2.16)

It remains to consider $G_2(\zeta)$ and $G_3(\zeta)$. Note first that their integrands are bounded in $\mathcal{B}$ except possibly near the origin, where we find, when $\zeta=0$,

$$G_2(0),\ G_3(0)\sim\frac{\zeta Q}{P^3}\int_0\frac{dq}{q}q^{d+2-3\sigma}\ . \tag{A10}$$

Provided the new condition

$$d>3\sigma-2\quad\text{or}\quad\sigma<\tfrac{1}{3}(d+2) \tag{A11}$$

is met, we thus have

$$G_2(\zeta)+G_3(\zeta)=I_d^0p'\zeta+o(\zeta)\ , \tag{A12}$$

where p' varies roughly as Q/P^3. This reconfirms the form (2.13) for $I_d(\zeta)$ but shows that the coefficient p as given in (2.16) should be corrected by the addition of p'. Since, however, even the sign of Q is not determined in general, we may still accept (2.16) as a rough estimate of p.

When the condition (A11) is *not* satisfied, the leading correction to the $p\zeta^{1/\gamma}$ term is no longer of order ζ. Rather, when $d<3\sigma-2$ one finds, by rescaling the integrands for G_2 and G_3 with $Pq^\sigma=\zeta y$ as before, that the term $q\zeta$ in (2.13) should be *preceded* by the new term

$$q^*\zeta^{(1/\gamma)+(2-\sigma)/\sigma}=q^*\zeta^{1-(3\sigma-2-d)/\sigma}>0\ , \tag{A13}$$

where $I_d^0q^*=Qc_{d,\sigma}/P^{(d+2)/\sigma}$, in which $c_{d,\sigma}$ is a sum of integrals depending only on d and σ.

It is evident that in this case the details of the analysis given in the main text must be changed, since the new term will play the role of $q\zeta$. In particular, any formula involving q (or $\bar p$ for $d\neq d_0$) needs modification. However, the methods that have been developed continue to apply, and all qualitative features must survive. Furthermore, the universal conclusions regarding the spectator phase boundary near the critical end point remain unchanged.

Finally, it is worth pointing out that although (A11) is relatively restrictive when $d=3$ or 2, necessitating $\epsilon\equiv(d-d_0)/\sigma>\frac{3}{10}$ or $\epsilon>0$, respectively, it represents no restriction at all on ϵ when $d\le 1$. (Recall that ϵ ranges from $-\frac{1}{2}$ to $+\frac{1}{2}$ as d varies from $d_-=\sigma$ to $d_+=2\sigma$: see also Fig. 3.)

---

*Present address: Instituto de Fisica, Universidade Federal do Rio Grande do Sul, Caixa Postal 15051, 91500 Porto Alegre, RS, Brazil.

[1]M. E. Fisher and M. C. Barbosa, Phys. Rev. B **43**, 11 177 (1991).

[2]It may be helpful to think of the nonordering field as the pressure: see Refs. 3 and 4.

[3]M. E. Fisher, in *Proceedings of the Gibbs Symposium, Yale University, May 1989,* edited by D. G. Caldi and G. D. Mostow (American Mathematical Society, Providence, 1990).

[4]M. E. Fisher and P. J. Upton, Phys. Rev. Lett. **65**, 2402 (1990); *ibid.* **65**, 3405 (1990).

[5]The distinction between the standard critical *exponents* α, β, and γ and the *phases* labeled with these symbols should always be clear from the context.

[6]M. E. Fisher, Physics **3**, 255 (1967); A. F. Andreev, Zh. Eksp. Teor. Fiz. **45**, 2064 (1963)[Sov. Phys. JETP **18**, 1415 (1964)]; S. N. Isakov, Commun. Math. Phys. **95**, 427 (1984).

[7]H. E. Stanley, Phys. Rev. **176**, 718 (1968).

[8]V. J. Emery, Phys. Rev. B **11**, 239 (1975); **11**, 3397 (1975).

[9]S. Sarbach and M. E. Fisher, Phys. Rev. B **18**, 2350 (1978). We denote this paper SF and follow its notation closely.

[10]M. E. Fisher and S. Sarbach, Phys. Rev. Lett. **41**, 1127 (1978); S. Sarbach and M. E. Fisher, Phys. Rev. B **20**, 2797 (1979).

[11]S. Sarbach and T. Schneider, Phys. Rev. B **16**, 347 (1977).

[12]See also I. D. Lawrie and S. Sarbach, in *Critical Phenomena and Phase Transitions,* edited by C. Domb and J. L. Lebowitz (Academic, New York, 1984), Vol. 9, p. 1.

[13]M. C. Barbosa (unpublished).

[14]See also G. S. Joyce, in *Phase Transitions and Critical Phenomena,* edited by C. Domb and M. S. Green (Academic, New York, 1972), Vol. 2, p. 375.

[15]It should be noted in this connection that SF (4.4) is not quite correct: the exponent d should be replaced by $d-\sigma$. However, this changes none of the subsequent analysis or general conclusions.

[16]The right-hand side of (3.14) vanishes at $\bar{\xi}=1$ (all ϵ) which, of course, is outside the region of validity of the approximation used for $I_d(\zeta)$. However, if one notes that $I_d(\zeta)=O(1/\zeta)$ as $\zeta\to\infty$, it is not hard to see that in an exact representation of the tricriticality equation, the right-hand side should still vanish when $\bar{\xi}$ increases, although only in the limit $\bar{\xi}\to\infty$; however that changes none of the qualitative conclusions.